RSC Advances

ROYAL SOCIETY OF CHEMISTRY

www.rsc.org/advances

RSC advances

ARTICLE

Effect of chain structure on the thermal conductivity of expanded graphite/polymer composites

Received 00th January 20xx,
Accepted 00th January 20xx

DOI: 10.1039/x0xx00000x

www.rsc.org/

Sha Deng [a], Jinwen Wang [a], Guiying Zong [a], Feng Chen [a,*], Songgang Chai [b], and Qiang Fu [a,*]

The thermal conductivity of expanded graphite (EG)/polymer composites is investigated in terms of polymer chain structures. The EG/polyphenylene sulfide (PPS) composite with backbone of benzene rings shows the continuously highest thermal conductivity and the fastest rate of enhanced ratio at the same content. Then it is followed by EG/syndiotactic polystyrene (sPS) composites with side groups of regularly arranged benzene rings. The last are the EG/ amorphous polystyrene (aPS) composites with side groups of randomly arranged benzene rings. Our results show that the chain structures of polymer matrices have a great influence on the interaction and crystallization of EG/polymer composites, which leads to the different thermal behavior. More precisely, the strong π-π interaction between EG and polymer, the nucleation of crystal at interface of EG/polymer and relatively rich EG content in the amorphous phase are benefit to enhancement of thermal conductivity. These factors are proved to be extremely important for designment of high thermal conductive composites in the fields of science and engineering.

1. Introduction

Nowadays, polymers based composite materials with high thermal conductivity have attracted increasing attention from both scientists and engineers, due to their extensive applications in electronic devices, electrical equipments and lighting[1-3]. By incorporating thermal conductive fillers into polymer, the thermal conductivity of composites can be improved remarkably. Up to now, there are a significant amount of related literatures investigating the effect of the kind, content, geometrical shape, size, combination, dispersion and interface of the fillers on the thermal conductivity of polymer composites[4-9].

Though the thermal conductivity of composites is generally codetermined by the fillers, matrices and interfaces, the studies on the effects of polymer matrices on the thermal conductivity of composites are quite limited. Haggenmueller et al. investigated the thermal conductivity of low-density polyethylene (LDPE) and high density polyethylene (HDPE) composites with various contents of SWCNT[10]. They found that the thermal conductivity of SWCNT/HDPE was much larger than that of SWCNT/LDPE at the same content, which evidenced a strong effect of polymer crystallinity and could possibly be explained by a reduction of the interfacial thermal resistance. However, the various chain structures of polymer matrices affect not only the crystal behavior of composites but also the interaction between the fillers and matrices, which has a great influence on the thermal conductivity of composites. Specially, numerous literatures have reported strong π-π interaction between carbon fillers and polymer with benzene rings or conjugated double bonds, such as graphene/PS[11], CNT/PPS[12] . Moreover, the polymers with different chain structures show various strengths of interaction with carbon fillers on account of the positions of the benzene rings and heterocyclic conjugated groups[13, 14]. For example, molecular dynamics (MD) simulation results have shown that the polymers with aromatic rings on the backbone (PmPV and poly(p-phenylenevinylene)) have stronger interaction with the SWCNT than those with side group of aromatic rings (polystyrene and poly(phenylacetylene)), as these aromatic rings on the polymer backbone are much easier to align parallelly to the nanotube surface and therefore provide strong interfacial adhesion[13]. However, few studies have been specialized on the effect of polymer chains with different positions of benzene rings on the thermal conductivity of polymer composites.

Poly (phenylene sulfide) (PPS) is a kind of rigid linear molecule with benzene-ring backbone structure, which makes it crystallize and have strong interaction with carbon series fillers. Syndiotactic polystyrene (sPS) and amorphous polystyrene (aPS) are polymers with side groups of benzene rings, which have relatively weak interactions with carbon based fillers. In general, sPS is partially crystalline because of the regularly arranged aromatic rings, while aPS is completely amorphous because the benzene rings are random distributed. EG/polymer composites with varying contents of EG are prepared by high speed solid-state rotation premixing, followed by internal melt mixing and compress molding, since melt processing is an economical and convenient method for most of thermoplastics. Our results show that chain structures of polymer matrices have significant influences on the thermal conductivity of composites and would make for the selection of fillers and matrices for high thermal conductivity of composites.

[a] College of Polymer Science and Engineering, State Key Laboratory of Polymer Materials Engineering, Sichuan University, Chengdu 610065, China.
[b] National Engineering Research Center of Electronic Circuits Base Materials, Guangdong Shengyi Technology Limited Corporation, Dongguan, 523039, China.
* Corresponding authors: Tel. +86-28-85405402,
E-mail address: fengchen@scu.edu.cn (F. Chen); qiangfu@scu.edu.cn (Q. Fu)

2. Experimental

2.1 Raw Materials

Amorphous polystyrene (aPS, PG33, 1.04 g/cm^3) was supplied by Sino-foreign Joint Venture Zhenjiang Qimei Chemical Co., Ltd. Syndiotactic polystyrene (sPS, SP130, 1.04g/cm^3) was purchased from Idemitsu Kosan Co., Ltd. Commercially available poly (phenylene sulfide) (PPS, PR06, 1.34 g/cm^3) was obtained from Chevron Phillips Chemical Company LP. The original graphite intercalation compounds (GICs, KP32) were acid-intercalated natural crystalline graphite, obtained from Qingdao Super Graphite Co, Ltd.

2.2 Filler and composite preparation

Before compounding, all the three original polymer granules were pulverized into powders and then screened to the similar sizes with wire mesh (60-100 eye/inch) to insure the same initial dispersion. The EG (2.26 g/cm^3) was prepared by putting GICs in a muffle furnace at 960 °C for 60 s. After rapid heating, the GICs were explosively expanded for hundreds of times along the c-axis direction and emerged an enormous increase in volume due to the evaporation of the intercalators.

The aPS and EG powders were firstly blended in the high-speed rotating mixer (Linda Mechanical Co., Ltd. China) at 25,000 rpm for 3 min. The EG contents in hybrids were controlled as 0, 5, 10, 15, 20, 30 and 40 wt%. The pre-dispersed EG/aPS powder hybrids were melted in an internal mixer (Rheocord 9000, haake Co., Ltd. Germany) operated at 60 rpm and 200 °C for 10 min. After being placed in a vacuum oven at 60 °C for 12 h, the as-prepared composites were compression molded (KT-0701, Beijin Kangsente Co., Ltd. China) at 200 °C and at low pressure（2 MPa）for 120 s (2 degassing cycles), then a high pressure（10 MPa）for 180 s followed by air cooling. The compression molded plates were cut into regular shape for conductivity measurement. The EG/sPS and EG/PPS composites were prepared by the same procedure except that the processing temperature was 290 °C and 300 °C, respectively. It should be noted that the processing temperatures for the three matrices are different because aPS is a kind of amorphous polymer whose glass transition temperature is 100℃ and processing temperature is 185-215 ℃, while semicrystalline sPS has a melting temperature (T_m) of 270℃, whose processing temperature is 280-300℃. As for PPS, T_m is 278℃ and proper processing temperature range is 290–327℃. Though the temperatures are not same, all the three polymer matrices show good flow property and are easy to be mixed with EG. For the convenient comparison of thermal conductivity in the three EG/polymer composites, the weight percentages of EG in composites were converted to volume percentages as displayed in Table. 1.

Table. 1 The conversion of weight content into volume content in EG/aPS, EG/sPS and EG/PPS composites.

Composites	Wt%	5	10	15	20	30	40
EG/aPS	Vol%	2.40	4.95	7.64	11.73	16.74	23.82
EG/sPS	Vol%	2.40	4.95	7.64	11.73	16.74	23.82
EG/PPS	Vol%	3.03	6.18	9.47	12.90	20.26	28.33

2.3 Material characterizations

The thermal conductivity was measured by a hot disk thermal analyzer (Hot Disk, Uppsala, Sweden). The measurement was performed with 30 mm×30 mm×3 mm bulk specimens which were cut from compression molded plates, by putting the sensor (3.189 mm diameter) between two similar slabs of material. The sensor supplied a heat pulse of 0.02-0.2 W for 20-5 s to the sample depending on the thermal conductivity of composites. The resistance was measured at room temperature with a Keithley 6487 picoammeter. The scanning electron microscopy (SEM) experiments were performed using an Inspect field-emission scanning electron microscope (FE-SEM, USA) instrument with an acceleration voltage of 20 kV to inspect the dispersion of EG in composites. Before SEM characterization, the cryo-fractured plates and powders were sputter-coated with gold. X-ray Diffraction (XRD) scans of aPS, sPS, PPS and their composites were carried out on a D/MAX-III X-ray diffractometer (DY1291, Philips, Holland) with Cu Kα radiation (K=0.1542 nm, where K is the wavelength of X-ray) at a generator voltage of 40 kV and current of 35 mA. The scanning speed was 9°/min, and the step size was 0.06° from 3 to 40°. Thermogravimetric Analysis (TGA) was conducted on a thermogravimetric analyzer (TG 209F1 Iris, Netzsch, Germany) under dry nitrogen. These samples were heated at a rate of 10°C /min, and the relative mass loss was recorded from 30°C to 600°C for EG/aPS and EG/sPS, 30°C to 800°C for EG/PPS. The Fourier transform infrared spectroscopy (FTIR) spectroscopic measurements were accomplished by a Thermo Nicolet FTIR microscope working at a resolution of 4 cm^{-1} and an accumulation of 32 scans. The crystal analysis was conducted on a Perkin-Elmer pyris-1 DSC calorimeter calibrated by indium. Around 5 mg specimens cut from the compression molded samples were directly heated from 50 °C to the desired temperature at a rate of 10 °C/min, held for 5 min to erase any thermal history and then cooled down to 50 °C at a rate of 10 °C/min. The melting enthalpy of the 100% crystalline sPS and PPS are 79.3 J/g[15] and 76.5 J/g[16], respectively.

2.4 Simulation Method

All the MD simulations were carried out using a commercial software package called Materials Studio developed by Accelrys Inc. The simulated models of the polymers were selected with comparable numbers of atoms and molecular weights (aPS 162 atoms, 1042; sPS 162 atoms, 1042; and PPS 112 atoms, 1082). Hence, the magnitude of the intermolecular interaction energy gave us a direct measure of the strength of their binding to the graphene sheets. The periodic supercell used in molecular dynamics simulations consists of one 10 nm*10 nm graphene platelet. Polymer chains were randomly distributed on the sides of the graphene sheets within a distance of 0.95 nm, which is the cutoff distance of van der Waals interactions. In this work, the condensed-phase optimized molecular potential for atomistic simulation studies (COMPASS) force field is used. The details of the force field have been described elsewhere [13]. All calculations were carried out in a vacuum condition using a constant number of particles, constant volume, and constant temperature (300K) ensembles without use of periodic boundary conditions. The Andersen thermostat was applied to control the temperature in this study. The interval of each MD simulation step was typically 1 fs.

3. Results and discussion

3.1 The thermal conductivity of EG/polymer composites

Fig.1 shows the thermal conductivity of EG/polymer composites as a function of EG volume contents. The thermal conductivities of the neat aPS, sPS, and PPS samples are 0.18, 0.23, and 0.24 W/mK, respectively. These indicate that crystalline polymers result in higher thermal conductivity, which is consistent with other studies [17, 18]. The EG/PPS composite shows the continuously highest thermal conductivity and the fastest rate of enhanced ratio at the same content throughout the whole range, then it is followed by EG/sPS composites, and the last are the EG/aPS composites.

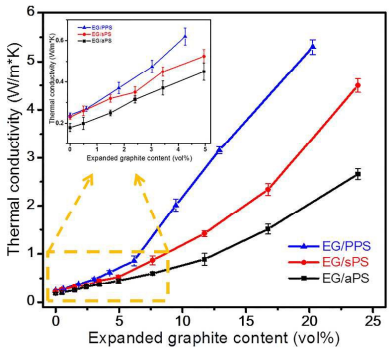

Fig.1 The thermal conductivity of EG/polymer composites as a function of EG volume contents (the error bar is marked).The inset shows the thermal conductivity at low content.

At low EG volume fractions, the thermal conductivities of EG/sPS and EG/aPS composites are increasing almost lineally and stay parallel with increasing EG content, whilst that of EG/PPS composite shows a slowly accelerated improvement. More precisely, the thermal conductivity of EG/sPS increases monotonically from 0.23 W/mK to 0.52 W/mK as the incorporation of EG reaching 4.95 vol%, while that of EG/aPS (0.45 W/mK at same content) is always slightly lower. In comparison, the improvement of thermal conductivity in EG/PPS (0.62 W/mK at 4.27 vol%) is obviously higher than the others. At the high EG volume fractions, the thermal conductivities of all three EG/polymer composites improve dramatically. But the rates of the enhanced ratios to the volume fraction remarkably depend on the nature of polymer matrices. The composite which displays the highest rate of the enhanced ratios is EG/PPS composites, exhibiting a marvellous increase to 5.15 W/mK at 20.26 vol%. Then it is followed by EG/sPS composite, which gradually increases to 4.50 W/mK at 23.82 vol%. For EG/aPS composite, the rate of the enhanced ratios is the lowest, which shows a moderate rise to 2.62 W/mK at 23.82 vol%.

The observed differences could be the result of polymer matrices with various chain structures, which may cause the differences of crystallizations and interactions of composites. So the dispersion of fillers, crystallization and interactions of composites should be characterized by further analysis of electrical conductivity, XRD, TGA, SEM, FIIR, DSC results and MD simulation.

3.2 The dispersion of EG in composites

It is widely known that electrical conductivity of composites is mainly dependent on the dispersion of fillers. So the dispersion of EG in the polymer matrices could be preliminarily investigated via the difference of electrical conductivity. The electrical conductivity at room temperature of the three polymer composites exhibits typical percolation behaviors, as shown in Fig.2. The electrically conductive pathways of composites are formed with increasing EG contents owing to enhanced probability of fillers contacts. As a result, the electrical conductivity of these composites increases from 10^{-8} to 102 S/m. And all the three composites have similar electrical conductivity at the same EG content, indicating comparable EG dispersion in the matrices.

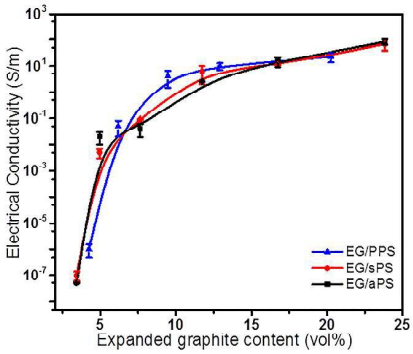

Fig.2 The electrical conductivity of three kinds of EG/polymer composites as a function of the EG volume contents (the error bar is marked).

The dispersion of EG in composites is further investigated by SEM characterization, as shown in Fig.3 and Fig.4. By using high speed solid-state mixing, the loose and porous vermicular structure of EG can be effectively destroyed and partly exfoliated, which makes it easy for EG to be adsorbed on the surface of the polymer powders and then form an efficient conductive network in the polymer matrix in the following internal melt mixing and compression molding. It is obvious that all three EG/polymer composites exhibit similar dispersion both at low and high EG content, that is, partial aggregates of EG form a network throughout the polymer matrix in macro scale and the exfoliated graphite nanosheets exhibit a homogeneous dispersion in micro scale. As demonstrated in Fig.3, EG is not sufficient to form thorough thermal conductive network and shows a discrete distribution in composites, leading to the linear increase of thermal conductivity of composites at low EG content. As EG content increases, it can be seen from Fig.4 that EG develops perfect thermal conductive networks both in macro and micro scale, resulting in a dramatical enhancement of thermal conductivity. However, the reason why the rates of the enhanced ratios to the volume fraction remarkably depend on the polymer matrices still remain unclear owing to the similar dispersion of EG in the three EG/polymer composites.

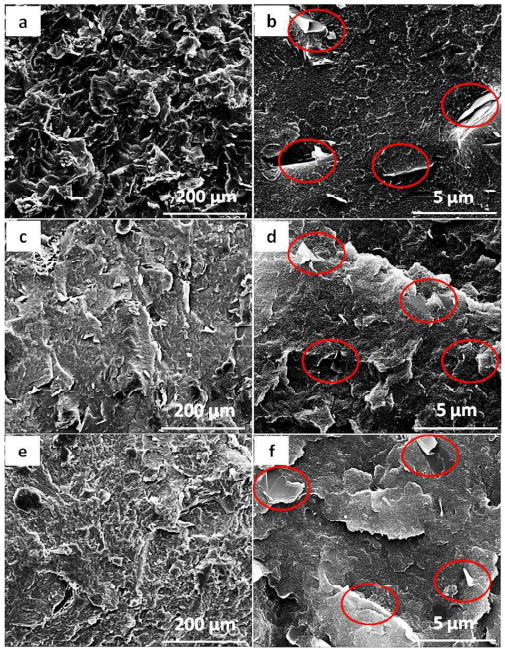

Fig.3 SEM images EG/aPS composite containing 10 wt% EG (a), (b); EG/sPS composite containing 10 wt% EG (c), (d); EG/PPS composite containing 10 wt% EG (e), (f). The red circles indicate the dispersion of graphite nanosheets.

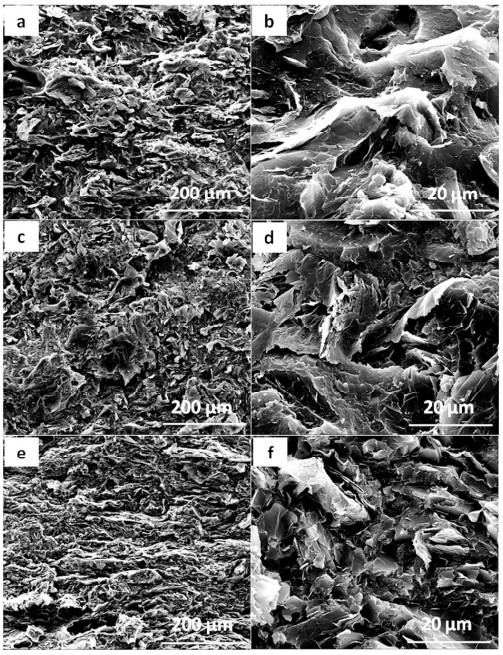

Fig.4 SEM images of EG/aPS composite containing 30 wt% EG (a), (b); EG/sPS composite containing 30 wt% EG (c), (d); EG/PPS composite containing 30 wt% EG (e), (f).

X-ray diffraction patterns of aPS, sPS, PPS and their composites obtained after compression molding are presented in Fig. 5. aPS shows no diffraction, while sPS and PPS show diffraction peaks corresponding to different planes of crystal. The sharp reflection peak at 2θ = 26.7°, corresponding to the plane of (002) in EG, appears in all curves of composites without any significant change in position [19]. This implies that even at strongly shearing conditions applied using high-speed rotating mixer and inner mixing, the full exfoliation of EG is difficult to achieve. In addition, the diffraction intensity increases with EG content owing to the presence of more platelets in a unit volume. The crystal structures of EG fillers and matrices have no evident influence on each other.

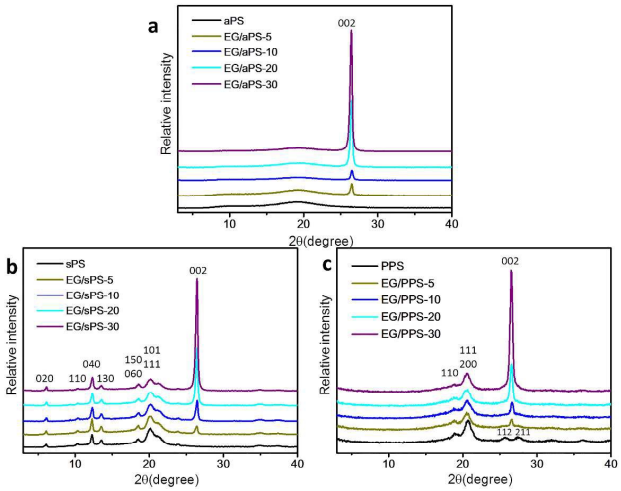

Fig.5 X-ray diffraction patterns of aPS, sPS, PPS and their composites.

In order to assess the thermal stability and the real content of PS, sPS, PPS and their composites, TGA was conducted. As shown in Fig. 6, all composites exhibit similar thermal degradation behaviour, compared to the matrices, indicating that the addition of EG does not change the thermal decomposition mechanism of the three matrices. The char yields of neat aPS, sPS and PPS were 0.211%, 0.2446% and 41.84%, respectively, so the real content of EG needs to be calculated as listed in Table 2. Although there is a slight difference between the real content and EG content we designed, they are within margin of error. In other words, the real EG content of composites is almost same as we designed, namely good dispersion by our processing method.

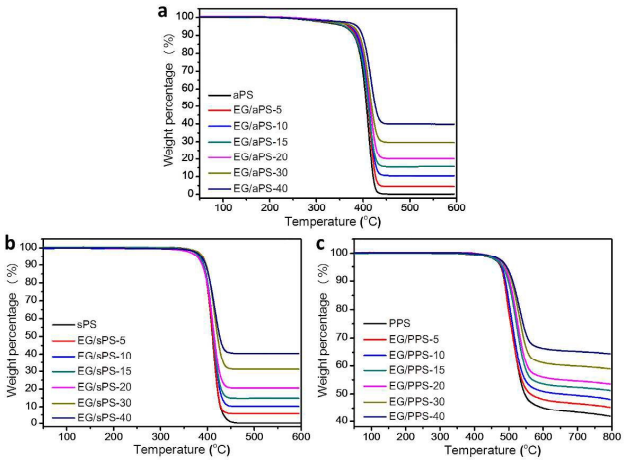

Fig.6 TGA thermograms of aPS, sPS, PPS and their composites.

Table.2 EG content calculated based on TGA characterization.

(wt %-D = EG content designed, wt %-T = Residual mass ratio obtained from TGA, wt %-Real = Real content of EG)

wt %-D	0	5	10	15	20	30	40
wt %-T of EG/aPS	0.211	4.475	10.5	15.71	19.7	29.56	39.86
wt %-Real in EG/aPS	0	4.273	10.31	15.53	19.53	29.41	39.73
wt %-T of EG/sPS	0.2446	5.638	10.4	14.68	20.75	31.12	40.46
wt %-Real in EG/sPS	0	5.40	10.18	14.47	20.55	30.95	40.31
wt %-T of EG/PPS	41.84	45.3	48.13	50.81	53.53	58.86	65.01
wt %-Real in EG/PPS	0	5.94	10.81	15.40	20.09	29.26	39.85

3.3 The effect of π-π interaction on the thermal conductivity

Fig.7 shows the FTIR characteristic absorption peaks of benzene ring of three EG/polymer composites change both in the intensity and positions, as the FTIR spectrum has been proved to be a useful tool to characterize the π-π interactions[20, 21]. It can be seen from Fig.7a and Fig.7b that the characteristic absorption peaks of benzene ring stretching mode of sPS at 1491 cm^{-1} and 1452 cm^{-1} [22] exhibit a small shift to lower wavenumbers (1489 cm-1 and 1450 cm-1, respectively), while that of aPS [21] display a similar shift but different changes of peak intensity, when EG contents reaches 30 wt%. As for EG/PPS composites, the characteristic absorption peak of the benzene ring stretching mode of PPS at 1573 cm^{-1} [23] exhibits a remarkable shift to lower wavenumber (1565 cm^{-1}) and the absorption intensity of peeks gradually decrease with increasing EG content. Compared with sPS and aPS composites, the absorption peaks of the benzene ring stretching mode of PPS appear a more obvious red shift. In other words, polymers with backbone of aromatic rings have stronger interactions with EG than the ones with side groups of aromatic rings.

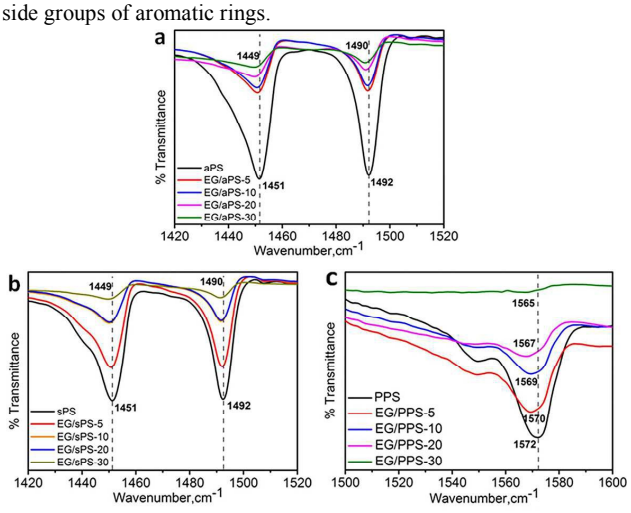

Fig.7 FT-IR spectra of EG/aPS composites in the range of 1420-1520 cm-1 (a); EG/sPS composites in the range of 1420-1520 cm-1 (b); EG/PPS composites in the range of 1500-1600 cm-1 (c).

Since MD simulation is another useful tool to characterize interaction between polymers and EG, the intermolecular interaction energy for the three models as a function of time are presented in Fig.8. Although all of the polymers have an obvious attractive interaction with EG, the specific chain structure plays a very important role in determining adhesion to EG. It is obvious that PPS has the strongest interaction with EG, and then sPS and aPS, which have comparable interactions with EG. Polymers with aromatic rings on the backbone are more easily arranged on the surface of graphene platelet, so the higher attractive interactions energies are directly attributed to the strong π-π interactions of their aromatic rings with the graphene platelet surface. Those are exactly consistent with FTIR results. As we know, previous studies have revealed that strong interactions between the filler and matrix lead to lower interfacial thermal resistance, which is a vital factor for improving thermal conductivity of polymer composites[6, 24, 25]. These may partly explain why EG/PPS composites exhibit the fastest rate of the enhanced ratios and continuously highest thermal conductivity at same content throughout the whole range. However, sPS and aPS composites show a different rate of the enhanced ratios and thermal conductivity despite of the same peak shift and similar attractive interactions energies, which need further structure analysis.

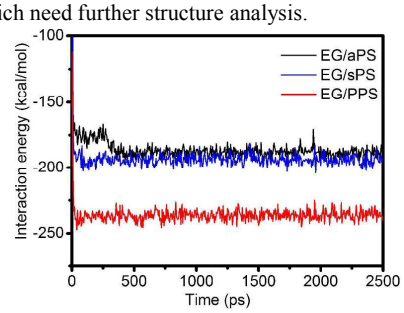

Fig.8 Intermolecular interaction energy between EG and polymers as a function of simulation time.

3.4 The effect of crystallization on the thermal conductivity

Traditionally, polymer crystallinity has a great influence on thermal conductivity, which approximately varies from 0.15 W/mK for amorphous polymers such as polymethylmethacrylate, to 0.5 W/mK for highly crystalline polymers such as high-density polyethylene[26, 27]. As for polymer composites, the increase of thermal conductivity in melt state is mainly related to the three-dimensional network of fillers, whereas the polymer crystallization is the dominating factor in solid state[5]. Fig.9 shows typical DSC crystal curves of the EG/sPS and EG/PPS composites with various EG contents and Table 3 displays their representative values of the melting temperature (T_m), the crystallization temperature (T_c), the melting enthalpy (ΔH_m) and the degree of crystallinity (χ_c). Both T_c of EG/sPS and EG/PPS composites show an obvious increase from 245.5 °C and 227.0 °C to 255.6 °C and 252.5 °C by adding 30 wt% EG, respectively, which indicates that EG can play the role of nucleating agent for sPS and PPS. However, the crystallinity decreases significantly from 43.3% to 33.6% for PPS, but slightly decreases for the sPS. The reason for the decreasing is that PPS with aromatic rings on the backbone has stronger interaction with EG than sPS with side groups of aromatic rings explained by FTIR and MD simulation discussed above, which

hinders the movement of molecular chain, thus preventing the crystallization of the polymer matrix[28]. In addition, the melt temperatures of EG/sPS and EG/PPS composites vary a little.

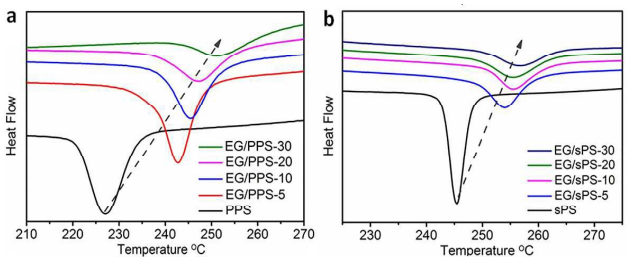

Fig.9 The typical DSC cooling curves of the EG/PPS and EG/sPS composites with various EG contents at a rate of 10 °C /min.

In fillers/semicrystalline composites, if fillers can provide nucleation sites for polymers, the interfacial thermal resistivity can be reduced and the thermal conductivity can be improved by increasing the nucleation of crystal at the fillers/polymer interface [10, 29]. Thus, we deduce that the interfacial thermal resistivity in both EG-sPS and EG-PPS is reduced, which is benefit to the thermal conductivity of related composites. In addition, it is reported when the conducting fillers are blended with insulating crystalline matrices, they show a more rapid increase in conductivity relative to blends prepared using amorphous matrices[30, 31]. The possible explanation is the relatively large crystalline domains may result in EG confinement in the amorphous phase, where high EG concentration may possibly be exploited to maximize EG-EG thermal contact. As a consequence, the thermal conductivity of EG/sPS composite is always higher than that of EG/aPS composite with completely amorphous structure.

Table.3 The representative crystallization values of EG/PPS and EG/sPS composites with various EG contents.

Composites	T_m (°C)	T_c (°C)	ΔH_m(J/g)	χ_c (%)
EG/PPS-0	280.0	227.0	33.1	43.3
EG/PPS-5	281.4	245.7	33.7	46.4
EG/PPS-10	280.9	247.5	30.6	44.6
EG/PPS-20	278.2	251.7	24.2	39.5
EG/PPS-30	278.1	252.5	18.0	33.6
EG/sPS-0	270.9	245.5	29.6	37.3
EG/sPS-5	271.3	254.4	27.3	36.2
EG/sPS-10	271.0	254.6	25.8	36.0
EG/sPS-20	270.1	254	21.6	34.0
EG/sPS-30	270.6	255.6	19.5	35.4

4. Conclusion

In summary, EG/aPS, EG/sPS and EG/PPS composites with various EG contents are prepared by high speed solid-state rotation premixing, followed by internal melt mixing and compress molding. The thermal conductivity of the three EG/polymer composites are dramatically improved but the rates of the enhanced ratios to the volume fraction remarkably depend on the chain structures of polymer matrices. These may result from the differences of interaction and crystallization of composites. Firstly, the polymer with backbone of benzene rings shows stronger π-π interactions between EG and PPS than the ones with the side groups of benzene rings, leading to lower interfacial thermal resistance. Secondly, the effective nucleation of EG could reduce the interfacial thermal resistivity and consequently improve the thermal conductivity by increasing the nucleation of crystal at the EG/polymer interfaces. In addition, the crystallization of polymer matrices exclude the EG in the amorphous phase, so the resulted relatively rich EG content in amorphous phase may possibly be exploited to maximize EG-EG thermal contact. Those factors show weak influences on trends of the thermal conductivity at low EG content, but obviously strong influences at high EG content. Our results clearly indicate that the thermal conductivity of polymer composites not only depends on filler content but also the chain structures of polymer matrices, which is crucial for the design of high thermal conductive polymer composites urgently needed in electronic and electric fields.

Acknowledgement

We would like to express our great thanks to the National Natural Science Foundation of China for financial support (Grant No. 51173112, 21274095 and 51573102). This work was also supported by Guangdong Shengyi Technology Limited Corporation (China).

Notes and references

1. G. Unsworth, N. Zamel and X. Li, *International Journal of Hydrogen Energy*, 2012, **37**, 5161-5169.
2 .H. Ji, D. P. Sellan, M. T. Pettes, X. Kong, J. Ji, L. Shi and R. S. Ruoff, *Energy & Environmental Science*, 2014, **7**, 1185-1192.
3. H. Zhu, Y. Li, Z. Fang, J. Xu, F. Cao, J. Wan, C. Preston, B. Yang and L. Hu, *ACS nano*, 2014, **8**, 3606-3613.
4. Z. Han and A. Fina, *Progress in Polymer Science*, 2011, 36, 914-944.
5. S. Laske, I. Duretek, A. Witschnigg, H. Mattausch, D. Tscharnuter and C. Holzer, *Polymer Engineering & Science*, 2012, **52**, 1749-1753.
6. J. S. Park, Y. J. An, K. Shin, J. H. Han and C. S. Lee, *RSC Adv.*, 2015, **5**, 46989-46996.
7. C. Seran, I. Hyungu and K. Jooheon, *Nanotechnology*, 2012, **23**, 065303.
8. S. Peddini, C. Bosnyak, N. Henderson, C. Ellison and D. Paul, *Polymer*, 2014, **55**, 258-270.
9. Z. Lin, A. Mcnamara, Y. Liu, K.-s. Moon and C.-P. Wong, *Composites Science and Technology*, 2014, **90**, 123-128.
10. R. Haggenmueller, C. Guthy, J. R. Lukes, J. E. Fischer and K. I. Winey, *Macromolecules*, 2007, **40**, 2417-2421.
11. B. Shen, W. Zhai, C. Chen, D. Lu, J. Wang and W. Zheng, *ACS Applied Materials & Interfaces*, 2011, **3**, 3103-3109.
12. S. Deng, Z. Lin, B. Xu, H. Lin and C. Du, *Polymer-Plastics Technology and Engineering*, 2014, **53**: 1590-1597.

13. M. Yang, V. Koutsos and M. Zaiser, *The Journal of Physical Chemistry B*, 2005, **109**, 10009-10014.
14. M. Foroutan and A. T. Nasrabadi, *The Journal of Physical Chemistry B*, 2010, **114**, 5320-5326.
15. C. H. Su, U. Jeng, S. H. Chen, C. Y. Cheng, J. J. Lee, Y. H. Lai, W. C. Su, J. C. Tsai and A. C. Su, *Macromolecules*, 2009, **42**, 4200-4207.
16. J. N. Hay and D. A. Luck, *Polymer*, 2001, **42**, 8297-8301.
17. L. Langer, D. Billaud and J.-P. Issi, *Solid State Commun*, 2003, **126**, 353-357.
18. V. Singh, T. L. Bougher, A. Weathers, Y. Cai, K. Bi, M. T. Pettes, S. A. McMenamin, W. Lv, D. P. Resler and T. R. Gattuso, *Nature nanotechnology*, 2014, **9**, 384-390.
19. L. Wang, Y. Cui, S. Yang, B. Li, Y. Liu, P. Dong, J. Bellah, G. Fan, R. Vajtai and W. Fei, *RSC Advances,* 2015, **5**, 19321-19328.
20. X. S. Du, M. Xiao and Y. Z. Meng, *Journal of Polymer Science Part B: Polymer Physics*, 2004, **42**, 1972-1978.
21. R. K. Goyal, P. A. Jagadalle and U. P. Mulik, *J Appl Polym Sci*, 2009, **111**, 2071-2077.
22. A. R. Albunia, P. Musto and G. Guerra, *Polymer*, 2006, **47**, 234-242.
23. R. Caminiti, L. D'Ilario, A. Martinelli, A. Piozzi and C. Sadun, *Macromolecules*, 1997, **30**, 7970-7976.
24. Y. Yao, X. Zeng, K. Guo, R. Sun and J.-b. Xu, *Composites Part A: Applied Science and Manufacturing*, 2015, **69**, 49-55.
25. J. Zhao, F. Du, W. Cui, P. Zhu, X. Zhou and X. Xie, *Composites Part A: Applied Science and Manufacturing*, 2014, **58**, 1-6.
26. J. Gu, N. Li, L. Tian, Z. Lv and Q. Zhang, *RSC Advances*, 2015, **5**, 36334-36339.
27. C. L. Choy, Polymer, 1977, 18, 984-1004.
28. J. Wei and J. Qiu, *Polymer*, 2014, **55**, 3818-3824.
29. D. Cai and M. Song, *Carbon*, 2008, **46**, 2107-2112.
30. A. R. Hopkins and J. R. Reynolds, *Macromolecules*, 2000, **33**, 5221-5226.
31. S. Pal, G. Balasubramanian and I. K. Puri, *The Journal of Chemical Physics*, 2012, **136**, 044901-044907.